Published April 9, 2012

Dendritic position is a major determinant of presynaptic strength

Arthur P.H. de Jong,[1] Sabine K. Schmitz,[1] Ruud F.G. Toonen,[1] and Matthijs Verhage[1,2]

[1]Department of Functional Genomics and [2]Department of Clinical Genetics, Center for Neurogenomics and Cognitive Research, VU University Amsterdam and VU Medical Center, 1081 HV Amsterdam, Netherlands

Different regulatory principles influence synaptic coupling between neurons, including positional principles. In dendrites of pyramidal neurons, postsynaptic sensitivity depends on synapse location, with distal synapses having the highest gain. In this paper, we investigate whether similar rules exist for presynaptic terminals in mixed networks of pyramidal and dentate gyrus (DG) neurons. Unexpectedly, distal synapses had the lowest staining intensities for vesicular proteins vGlut, vGAT, Synaptotagmin, and VAMP and for many nonvesicular proteins, including Bassoon, Munc18, and Syntaxin. Concomitantly, distal synapses displayed less vesicle release upon stimulation. This dependence of presynaptic strength on dendritic position persisted after chronically blocking action potential firing and postsynaptic receptors but was markedly reduced on DG dendrites compared with pyramidal dendrites. These data reveal a novel rule, independent of neuronal activity, which regulates presynaptic strength according to dendritic position, with the strongest terminals closest to the soma. This gradient is opposite to postsynaptic gradients observed in pyramidal dendrites, and different cell types apply this rule to a different extent.

Introduction

Presynaptic terminals in the central nervous system, even those formed by a single neuron, form a highly heterogeneous population in terms of both structure and function. Ultrastructural analysis of hippocampal synapses revealed a wide range in the number of synaptic vesicles (40–800 per terminal) and the number of morphologically docked vesicles (0–15 per terminal; Murthy et al., 2001; Schikorski and Stevens, 2001; Branco et al., 2010). A similar variation was observed using functional readouts, including synaptic release probability (p_r; Murthy et al., 1997; Slutsky et al., 2004; Branco et al., 2008; Matz et al., 2010) and the number of release-ready vesicles (the readily releasable vesicle pool [RRP]; Murthy et al., 2001; Matz et al., 2010). The p_r can change rapidly over time as a result of repetitive stimulation (i.e., short-term plasticity [STP]). The direction of change (facilitation or depression) and the extent of STP depend to a large extend on the initial p_r and the RRP size and are therefore synapse specific as well (Dobrunz and Stevens, 1997; Murthy et al., 1997). Indeed, presynaptic terminals from a single neuron express different types of STP (Reyes et al., 1998; Scanziani et al., 1998; Koester and Johnston, 2005). In addition, each terminal expresses a unique range of presynaptic receptors. Over 70 presynaptic receptors have been described so far, and most of these receptors modulate p_r and STP, via the activation of intracellular signal transduction pathways (de Jong and Verhage, 2009). These forms of synaptic heterogeneity largely increase the computational power of a neuronal network, as every terminal acts as an independent information-processing unit (Abbott and Regehr, 2004; Branco and Staras, 2009).

Over the recent years, it has become increasingly clear that many of these presynaptic characteristics depend on the dendrite on which the terminal is formed. In hippocampal neurons in vitro, neighboring synapses have similar p_r (Murthy et al., 1997; Welzel et al., 2010), which is thought to be specific for a dendritic branch (Branco et al., 2008). In slices, p_r and STP depend on the identity of the postsynaptic cell (Reyes et al., 1998; Scanziani et al., 1998; Koester and Johnston, 2005). Furthermore, the expression of presynaptic receptors depends on synapse

Correspondence to Matthijs Verhage: matthijs.verhage@cncr.vu.nl

Abbreviations used in this paper: AP, action potential; AP5, (2R)-amino-5-phosphonovaleric acid; DG, dentate gyrus; DIV, day in vitro; DNQX, 6,7-dinitroquinoxaline-2,3-dione; EPSP, excitatory postsynaptic potential; MAP, microtubule-associated protein; P/D, proximal/distal; p_r, release probability; RRP, readily releasable pool; STP, short-term plasticity; SypHy, synaptophysin-phluorin; TTX, tedrodoxin.

Supplemental Material can be found at:
http://jcb.rupress.org/content/suppl/2012/04/05/jcb.201112135.DC1.html
http://jcb.rupress.org/content/suppl/2012/04/30/jcb.201112135.DC2.html

The Rockefeller University Press $30.00
J. Cell Biol. Vol. 197 No. 2 327–337
www.jcb.org/cgi/doi/10.1083/jcb.201112135

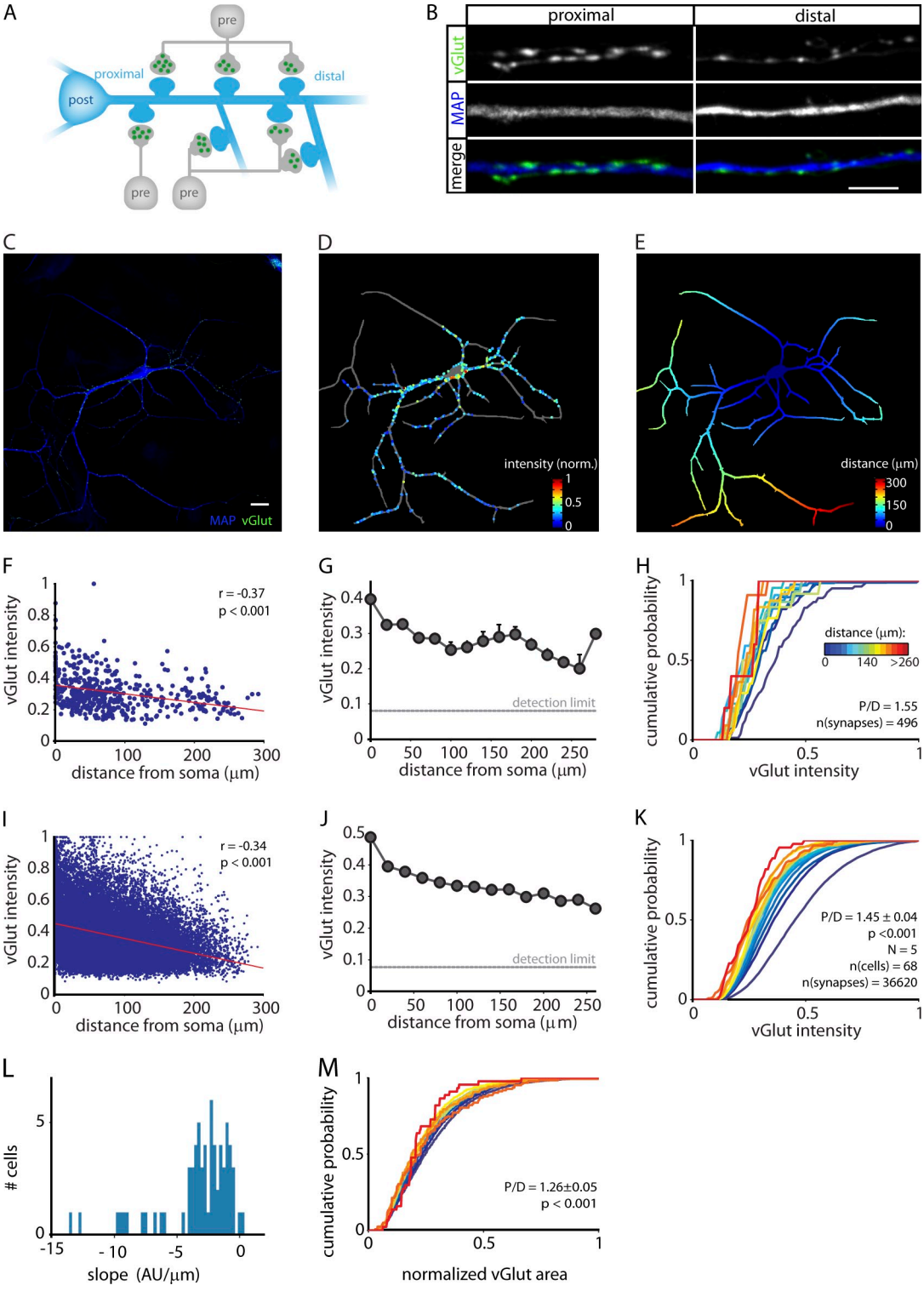

Figure 1. **Synapse location determines the amount of vesicles per terminal.** (A) Experimental design. A postsynaptic neuron (post) receives presynaptic input from multiple surrounding presynaptic neurons (pre). The vGlut staining intensity is used as a measure for the number of vesicles per presynaptic terminal (green). Note that a single presynaptic neuron may form multiple synapses along the dendritic tree. (B) Typical example of a proximal and distal dendrite stained for vGlut and MAP. Bar, 5 µm. (C) Example of an image used for analysis. Bar, 20 µm. (D) Analysis of the image in C. The detected neurites are shown in gray. Neurites from neighboring neurons are omitted from the analysis. The dots represent detected synapses, with their vGlut intensity color coded. The intensity was normalized (norm.) to the most intense synapse detected in this neuron. The size of the dots does not represent the surface area of the detected synapse. (E) Distance mask of the neuron in C used for distance measurements of the detected synapses. Distance was measured along the MAP staining and, thus, takes into account the morphology of the dendritic tree. (F–H) Different methods to plot the results of the analysis in B–D. (F) Relationship between distance from the soma and vGlut intensity. Each dot represents an individual synapse, and the solid line shows a linear fit through the data. Inset displays the Spearman correlation coefficient (r) and significance (p-value). (G) Same data as in F, averaged in bins of 20 µm. Error bars represent SEM. (H) Cumulative histograms of the data in F, in bins of 20 µm. The color of each line indicates the distance from the soma. The legend also

location, both in slices (Shigemoto et al., 1996; Scanziani et al., 1998; Pelkey et al., 2006) and in culture (Laviv et al., 2010).

The postsynaptic gain, in turn, is largely dependent on the dendritic position of the synapse. In hippocampal pyramidal cells, distal synapses express an increased number of AMPA receptors, leading to larger local postsynaptic currents (Magee and Cook, 2000; Smith et al., 2003). In addition, synchronous input on distal synapses of hippocampal and cortical pyramidal cells can be amplified by supralinear summation of excitatory postsynaptic potentials (EPSPs) and the initiation of dendritic calcium spikes (Losonczy and Magee, 2006; Branco and Häusser, 2011). Dendritic location is therefore thought to be of crucial importance for the integration of synaptic input (Sjöström et al., 2008). It can be predicted that presynaptic terminals contribute to this amplification by the formation of stronger presynaptic inputs at more distal dendritic positions.

In the current study, we investigate the general relationship between presynaptic strength and the dendritic position of the synapse. Surprisingly, we did not observe the expected increase in presynaptic strength with increasing distance from the postsynaptic soma. In contrast, we found that in both inhibitory and excitatory synapses, the number of synaptic vesicles and the local concentration of presynaptic proteins are highest at synapses formed close to the soma. This clearly affected vesicle release because proximal synapses had a larger RRP. Strikingly, this distance-dependent scaling of presynaptic strength was insensitive to manipulations of neuronal activity and was dependent on the identity of the postsynaptic neuron. These results reveal a novel, cell-wide rule that determines the strength of presynaptic input along the dendritic tree. We believe that this will have profound implications for the integration of neuronal activity.

Results

The number of synaptic vesicles depends on synapse location

We analyzed the amount of vesicles per presynaptic terminal as a function of its location on the dendrite relative to the soma. Cultured hippocampal neurons were stained with antibodies against the vesicular glutamate transporter vGlut (Fig. 1, A–C). We consider vGlut intensity a reliable measure for the relative amount of synaptic vesicles because the number of vGlut copies per vesicle is tightly controlled (Mutch et al., 2011). Furthermore, only ∼1% vGlut is expressed at the cell surface (Balaji and Ryan, 2007). For every synapse, we measured the vGlut intensity and its distance from the postsynaptic soma along the dendritic marker microtubule-associated protein (MAP; Fig. 1, C–E). Surprisingly, we found a near perfect gradient of vGlut levels, with proximal synapses having the highest intensity (Fig. 1, F–K). The median normalized intensity dropped from 0.50 at the soma to 0.24 at 250 µm from the soma. Note that considerable variation exists in intensity, even among synapses at similar distances, but that high intensity synapses are more likely to be found close to the soma (Fig. 1, I–K). However, even when binned and shown for individual neurons, a clear relation between distance and intensity of presynaptic staining was observed (Fig. 1, F–H).

To test to what extent the distance dependence of staining intensity holds for every individual neuron, we made linear line fits through the data of each neuron. In 66 of the 68 cells tested, this fit had a negative slope, indicating that all but two cells showed decreased vGlut intensity at distal sites (Fig. 1 L). Fig. 1 L also shows that some heterogeneity probably exists on either side of the median among different cell types in a mixed culture (Fig. 1 L and see final paragraph of Results). To further quantify the effect per cell, we calculated the ratio of proximal (<50 µm) over distal (last 50 µm) per cell. This proximal/distal (P/D) ratio was 1.45 ± 0.04 with $P < 0.001$ (one-sample Wilcoxon rank test), again indicating that individual cells display a distance-dependent decline in vGlut intensity. The differences in surface area of vGlut puncta between proximal and distal terminals were much smaller but still significant (median normalized area at the soma = 0.25; median area at 250 µm = 0.21; Fig. 1 M). It should be noted that, because of the lower vGlut intensity at distal synapses, the area measurements at distal terminals are less precise. These results suggest that the number of vesicles per terminal, and to a lesser extent the physical dimensions of the terminal, depend on the dendritic position of the synapse.

To test whether the observed gradients reflect a certain developmental stage rather than a stable state, we compared sister cultures fixed at 14 or 21 d in vitro (DIV). Despite significant differences in mean synapse area and synapse density, we did not find any difference in the distance dependency of the vGlut intensity of synapse area (Fig. S1). Thus, the distance dependency of vGlut intensity is stable once mature synapses are formed.

Protein content of presynaptic terminals depends on synapse location

Next, we tested the distance dependency of the levels of a range of other presynaptic proteins with immunocytochemistry (Fig. 2). Synapses were detected with vGlut, Synapsin, vGAT, or VAMP, and the detected regions were subsequently used to quantify the synaptic levels of other proteins. We observed a distance-dependent decline in the levels of the vesicular γ-aminobutyric acid transporter vGAT, which was similar to vGlut (Fig. 2 B). This suggests that the number of vesicles of excitatory and inhibitory synapses is equally dependent on synapse location. Furthermore, similar gradients were found for the presynaptic scaffolding protein Bassoon and for Munc18, VAMP, Synaptotagmin-1, and Syntaxin, which are core proteins of the vesicle release machinery (Fig. 2, A and B; Sudhof, 2004). Similar to our results with vGlut stainings (Fig. 1), we found only a small drop in surface area at more distal synapses for terminals

applies to K and M. P/D is the ratio of proximal (<50 µm) over distal (last 50 µm). (I–K) Results from the complete vGlut dataset (n = 68 cells and 336,620 synapses). (I) Relationship between distance from soma and vGlut intensity. Each dot represents an individual synapse, and the solid line shows a linear fit through the data. (J) Same data as in I, averaged in bins of 20 µm. Error bars are too small to be seen. (K) Cumulative histograms of the data in I. P-value is the significance of the P/D ratio (one-sample Wilcoxon rank test). (L) Histogram of the slopes of linear line fits through data of individual cells. (M) Cumulative histograms of synapse surface area. AU, arbitrary unit; N, number of experiments.

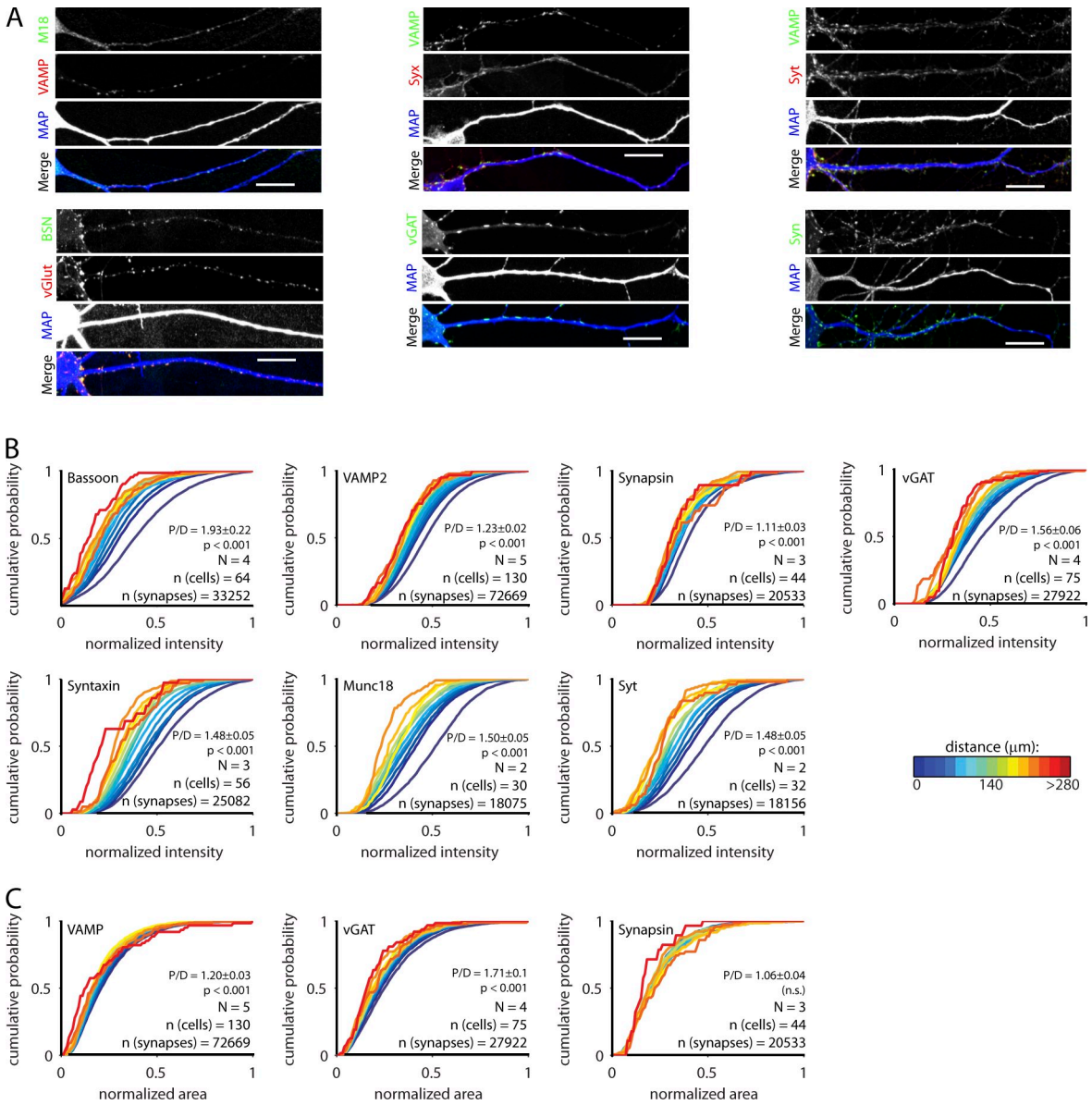

Figure 2. **Levels of proteins involved in secretion depend on synapse location.** (A) Example images of hippocampal network cultures stained for dendrite marker MAP and presynaptic proteins. Bars, 20 µm. (B) Cumulative histograms of the synaptic intensity of proteins involved in vesicle release. Synapses were grouped based on their distance from the postsynaptic soma. All intensities were normalized to the largest value per cell. P/D is the ratio of proximal (<50 µm) over distal (last 50 µm), and p-value is the significance of the P/D ratio. N represents the number of independent experiments. (C) Surface area of vGAT and VAMP puncta. BSN, Bassoon; M18, Munc18; Syn, Synapsin; Syt, Synaptotagmin; Syx, Syntaxin.

detected with vGAT, Synapsin, or VAMP (Fig. 2 C). Hence, the number of vesicles and the abundance of the release machinery in a terminal depend on its dendritic location.

RRP size depends on synapse location

Next, we tested whether the correlation between protein levels and synapse position translates to functional differences in synaptic release properties. We transfected a fraction of the neurons in the network with synaptophysin-phluorin (SypHy), a fluorescent reporter of synaptic vesicle release (Granseth et al., 2006). We made electrophysiological recordings of a pair of neurons, of which one was SypHy transfected (which we refer to as the presynaptic cell), and one was a connected, untransfected cell (referred to as the postsynaptic cell). The postsynaptic cell was filled with Alexa Fluor 468 via the recording pipette to observe its morphology (Fig. 3, A and C). To determine the size of the RRP, we stimulated the presynaptic cell with 40 action potentials (APs) at 20 Hz (a stimulation protocol that is routinely used to probe the RRP; Schikorski and Stevens, 2001; Burrone et al., 2006; Matz et al., 2010) and measured the increase in fluorescence in every terminal in the field of view (Fig. 2 B). The cells where then fixed and analyzed with a confocal microscope to identify the terminals formed on the postsynaptic cell (Fig. 3 D). The RRP size of these synapses followed a skewed distribution (Fig. 3 E), in good agreement with previous studies (Murthy et al., 1997; Matz et al., 2010).

In line with our data on presynaptic protein content, we found that proximal synapses had a larger RRP than distal

synapses (Fig. 3 F). The median normalized RRP size ranged from 0.39 for synapses at the soma to 0.19 for synapses formed at >160 µm from the soma. The P/D ratio per cell was 1.55 ± 0.19 ($P < 0.01$). Furthermore, application of 50 mM NH_4^+ (which dequenches SypHy in unreleased vesicles; Miesenböck et al., 1998) confirmed the relationship between the number of vesicles and synapse position that we observed in fixed neurons (P/D ratio = 1.15 ± 0.18, $P < 0.01$; Fig. S2). These results indicate that the increased vesicle number and release machinery abundance translate into larger releasable vesicle pools in nerve terminals at proximal dendritic positions.

Distance dependency of presynaptic strength is independent of network activity

Previous studies have shown that neuronal activity fine tunes synaptic strength (Murthy et al., 2001; Turrigiano, 2008; Matz et al., 2010; Pozo and Goda, 2010) and, for synapses onto single dendritic branches, reduces the heterogeneity in p_r (Branco et al., 2008). Furthermore, manipulations of network activity alter synaptic protein levels (Matz et al., 2010; Lazarevic et al., 2011). The distance-dependent scaling of presynaptic strength could be caused by local differences in dendritic activity, which causes homeostatic adaptations of p_r (Branco et al., 2008). We therefore tested the effect of blocking AP firing with tedrodoxin (TTX) or blockage of excitatory synaptic transmission with 6,7-dinitroquinoxaline-2, 3-dione (DNQX) and (2R)-amino-5-phosphonovaleric acid (AP5) on distance-dependent scaling of presynaptic terminals. TTX or DNQX and AP5 were added at DIV 7, and samples were fixed at DIV 14 (Fig. 4 A). Both treatments had a substantial effect on mean synapse size and vesicle content (Fig. 4, B–D) as previously observed (Murthy et al., 2001; Branco et al., 2008; Lazarevic et al., 2011), but the correlation between vGlut intensity and synapse position remained (Fig. 4 E). In line with this observation, we did not find any significant differences in the P/D ratio per cell ($P = 0.81$; Fig. 4 F) or in the slope of the linear line fit per cell ($P = 0.94$; Fig. 4 G).

To further test the effect of network activity, we measured the distance dependency of presynaptic protein levels in autaptic islands. These neurons are grown in complete isolation and, thus, are devoid of network activity (Bekkers and Stevens, 1991). Furthermore, because all presynaptic terminals on an island are formed by the same axon, every synapse is expected to receive a similar activity pattern. This type of culture is routinely used to study presynaptic function (see for instance Murthy et al., 1997; Toonen et al., 2006; Jockusch et al., 2007). In these autaptic cultures, we found distance-dependent gradients for all presynaptic proteins tested, both vesicular and nonvesicular, in a similar fashion as observed in network cultures (Fig. 5). Thus, the dependence of vesicle number and secretion machinery abundance on dendritic position is independent of synaptic activity or differences in local postsynaptic current amplitude.

Protein levels are not correlated in an individual synapse

If the local concentration of release machinery proteins is indicative for presynaptic strength, it could be predicted that their levels

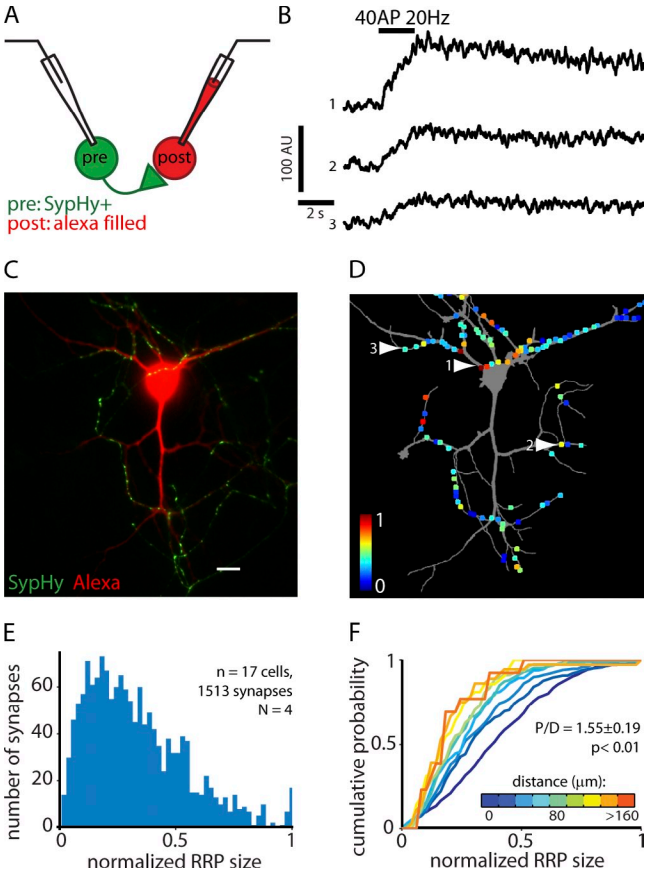

Figure 3. **RRP size depends on synapse location.** (A) Experimental design. pre, presynaptic; post, postsynaptic. (B) Example traces of synaptic SypHy fluorescence upon stimulation to release the RRP. (C) Example image of an Alexa Fluor–filled neuron receiving synaptic input from a SypHy+ cell. The SypHy image was taken in the presence of 50 mM NH_4^+. Bar, 20 µm. (D) Neurite mask of the neuron in C (gray) with all SypHy+ synapses formed on this neuron. RRP size is color coded. Arrows indicate synapses from which the traces in B were obtained. (E) Histogram of RRP size. (F) Cumulative histogram of the RRP sizes in E, grouped on synapse location. AU, arbitrary unit; N, number of experiments.

are correlated at the level of individual synapses. We therefore tested whether such a correlation exists within the costainings described in Figs. 2 and 5. As can be expected, the levels of vesicular proteins showed a good correlation: Spearman correlation coefficient (r) of VAMP versus Synaptotagmin = 0.59, and VAMP versus Rab3 r = 0.74. Furthermore, Bassoon intensities correlated well with Synapsin (r = 0.63) and vGlut (r = 0.61), whereas Rab3-interacting molecule and Synapsin showed a weaker correlation (r = 0.46). However, VAMP levels had almost no correlation with either Munc18 (r = 0.29) or Syntaxin (r = 0.22). These results show that although these proteins display a distance-dependent effect on the population level, differences between individual proteins of the release machinery exist in individual synapses.

Distance-dependent scaling is strongly reduced in dentate gyrus (DG) granule cells

Our data suggest that the previously observed increased postsynaptic gain at distal synapses (Magee and Cook, 2000; Losonczy and Magee, 2006) is counterbalanced by weaker presynaptic inputs. Interestingly, it was shown that dendrites of granule cells

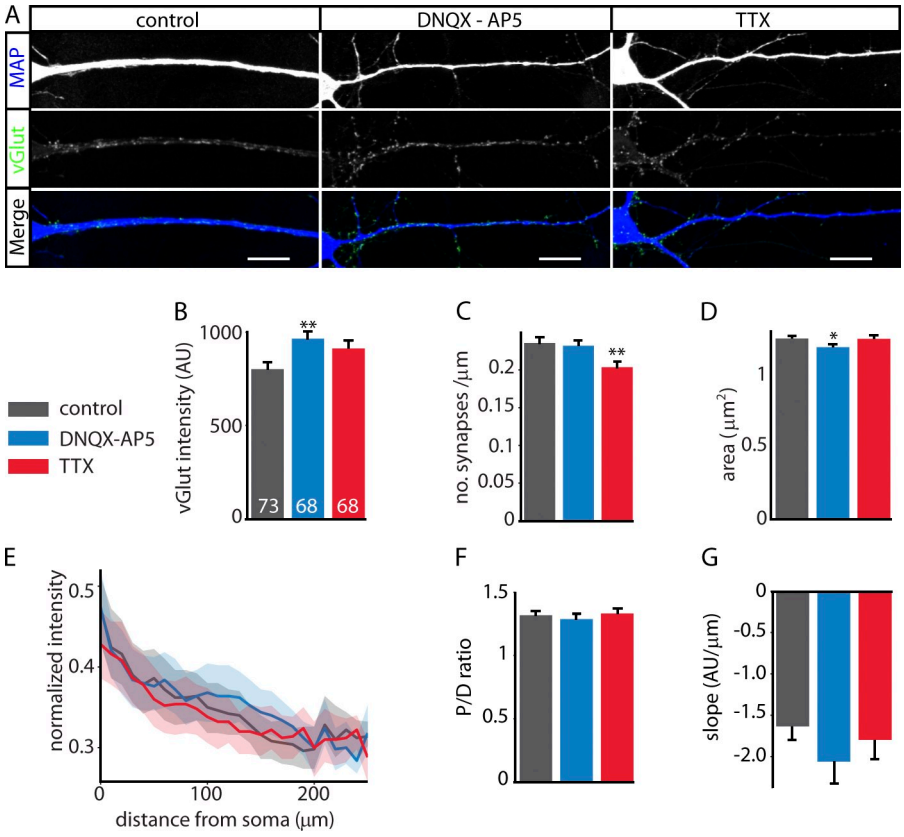

Figure 4. **Neuronal activity does not affect distance-dependent scaling of vGlut intensity.** (A) Example images of neurons treated for 7 d with DMSO (control), 10 µM DNQX and 50 µM AP5 (DNQX-AP5), or 2 µM TTX. Bars, 20 µm. (B) Mean synaptic vGlut intensity. Numbers refer to the number of observations. (C) Synapse density (number of synapses per micrometer of dendrite). (D) Surface area of vGlut puncta. (E) Distance dependency of vGlut after DNQX-AP5, TTX, or control. Solid lines represent the median normalized intensity, and the shaded area shows the 0.4–0.6 boundaries (see also Fig. S1). (F) P/D ratio of vGlut intensity. (G) Average slopes of linear line fits through data from individual neurons. Error bars represent means ± SEM. Control: $n = 73$ and 34,724 synapses; DNQX-AP5: $n = 68$ and 36,723 synapses; TTX: $n = 68$ and 27,417 synapses; $n = 3$. *, $P < 0.05$; **, $P < 0.01$ compared with control. AU, arbitrary unit.

in the DG integrate synaptic input independent of synapse location (Krueppel et al., 2011). We hypothesized that if distance-dependent scaling of presynaptic strength is important for the integration of synaptic input, pyramidal and DG cells might also scale their synaptic input differently. Previous work has shown that hippocampal neurons retain their morphological and functional characteristics in culture (Baranes et al., 1996; Tong et al., 1996; Williams et al., 2011). DG cells can be identified in culture using antibodies against the transcription factor Prox1; the remaining cell population (non-DG cells) consists of pyramidal cells from the cornu ammonis and a small fraction of interneurons (Bagri et al., 2002; Williams et al., 2011). We confirmed the specificity of Prox1 by morphological analysis of DG and non-DG cells. Comparable with in vivo (Seress and Pokorny, 1981; Claiborne et al., 1990; Kress et al., 2008), DG cells in culture had a smaller soma and a smaller and less complex dendritic tree (Fig. S3, A–H). We then quantified the vGlut intensity to measure distance-dependent scaling in both cell populations (Fig. 6). In non-DG cells, we found a strong reduction of vGlut intensity in more distal synapses (normalized median intensity at the soma = 0.39; median intensity at 260 µm = 0.26), consistent with our previous experiments (Fig. 6 B). Strikingly, distance-dependent scaling was strongly reduced in DG cells (normalized intensity at the soma = 0.39; normalized intensity at 260 µm = 0.31; Fig. 6, C and D). Even though proximal synapses were still slightly more intense than distal synapses (P/D ratio = 1.15 ± 0.06, $P < 0.001$), this was significantly smaller compared with non-DG cells ($P < 0.01$; Fig. 6 E). To further test this, we made line fits through the data of individual neurons. The slope of these fits was significantly smaller in DG cells ($P < 0.01$; Fig. 6 F), again indicating that distance-dependent scaling is reduced in these cells. The difference between both groups was even more pronounced when comparing absolute vGlut intensities (median intensity soma vs. distal = 706.6 vs. 409.1 arbitrary units [non-DG] and 518.1 vs. 690.8 arbitrary units [DG]); Fig. S3, I and J). These results suggest that populations of neurons that display different dendritic integration principles also have different rules for distance-dependent scaling of presynaptic input.

Discussion

It is well established that the number of vesicles, release machinery abundance, and p_r can vary widely between presynaptic terminals (Murthy et al., 1997; Schikorski and Stevens, 2001; Lazarevic et al., 2011). Because the regulation of presynaptic efficacy is a crucial element in neuronal information processing and memory formation (Abbott and Regehr, 2004), the strength of presynaptic terminals is expected to be dictated by tight rules. In cortical and hippocampal pyramidal neurons, the local amplitude and integration rules of postsynaptic currents are controlled by synapse location on the dendrite, with distal synapses having the highest gain (Magee and Cook, 2000; Losonczy and Magee, 2006). We predicted a similar rule for the strength of presynaptic input, to further amplify the signal of distal synapses. Surprisingly, we found the exact opposite.

Presynaptic strength depends on the location of the synapse

The synaptic levels of the vesicular proteins vGlut, vGAT, Synaptotagmin, and VAMP decreased with increasing distance from the postsynaptic soma (Figs. 1 and 2), from which we conclude that distal synapses have less vesicles. If vesicles at distal synapses contained fewer copies of these proteins, that might also contribute to these distance-dependent differences in staining intensity. However, this is unlikely because synaptic vesicles actively and rapidly mix between different presynaptic terminals via axonal transport (Fernandez-Alfonso and Ryan, 2008; Branco et al., 2010; Herzog et al., 2011), and single-vesicle quantification of vesicle content showed that the number of vGlut and Synaptotagmin molecules per vesicle shows little variation (Mutch et al., 2011). In addition to differences in the number of vesicles per terminal, we found similar distance-dependent differences in the local concentration of nonvesicular proteins essential for synaptic vesicle release (Figs. 2 and 5).

At the level of individual synapses, we observed moderate correlations in the levels of various vesicular proteins and of scaffold proteins and vesicular markers. However, the levels of other release machinery proteins did not correlate well. Thus, although the concentrations of these proteins show a distance-dependent effect on the population level, large differences between individual proteins do occur in single synapses. In most experiments described here, presynaptic terminals on a given dendrite originate from several neighboring neurons. As each presynaptic neuron has its independent gene expression program, the relationship between the expression of different presynaptic proteins is expected to be different in different subsets of presynaptic terminals. Furthermore, recent studies showed that in response to neuronal activity, synaptic levels of specific proteins are regulated, whereas other proteins are unaffected (Jiang et al., 2010; Lazarevic et al., 2011). For these reasons, the levels of various presynaptic proteins are not expected to show strong correlations.

The distance-dependent regulation of the number of vesicles and release machinery proteins probably accounts for the distance dependency of the RRP size (Fig. 3). Indeed, alterations in Munc18 and Bassoon levels are known to correlate with changes in RRP size (Toonen et al., 2006; Matz et al., 2010). Because the size of the RRP is a primary determinant of p_r and STP (Dobrunz and Stevens, 1997; Murthy et al., 1997), these differences in RRP size will have a profound effect on vesicle release during neuronal activity.

The data described here seem in conflict with previous studies, which did not find a relationship between p_r or RRP size and distance from the postsynaptic soma (Smith et al., 2003; Branco et al., 2008). Our results display a broad heterogeneity in RRP size, vesicle number, and protein levels, even between synapses with a similar distance from the soma (Figs. 1–3). This variation will make a distance-dependent effect on presynaptic strength hard to detect using low throughput methods. In our SypHy experiments, we were able to measure the RRP size of 1,513 synapses from 17 cells. With this relatively large number of synapses per cell, we observed a clear distance-dependent decline in RRP size (Fig. 3). The apparent discrepancy between previous studies and our results might thus be caused by an increased power

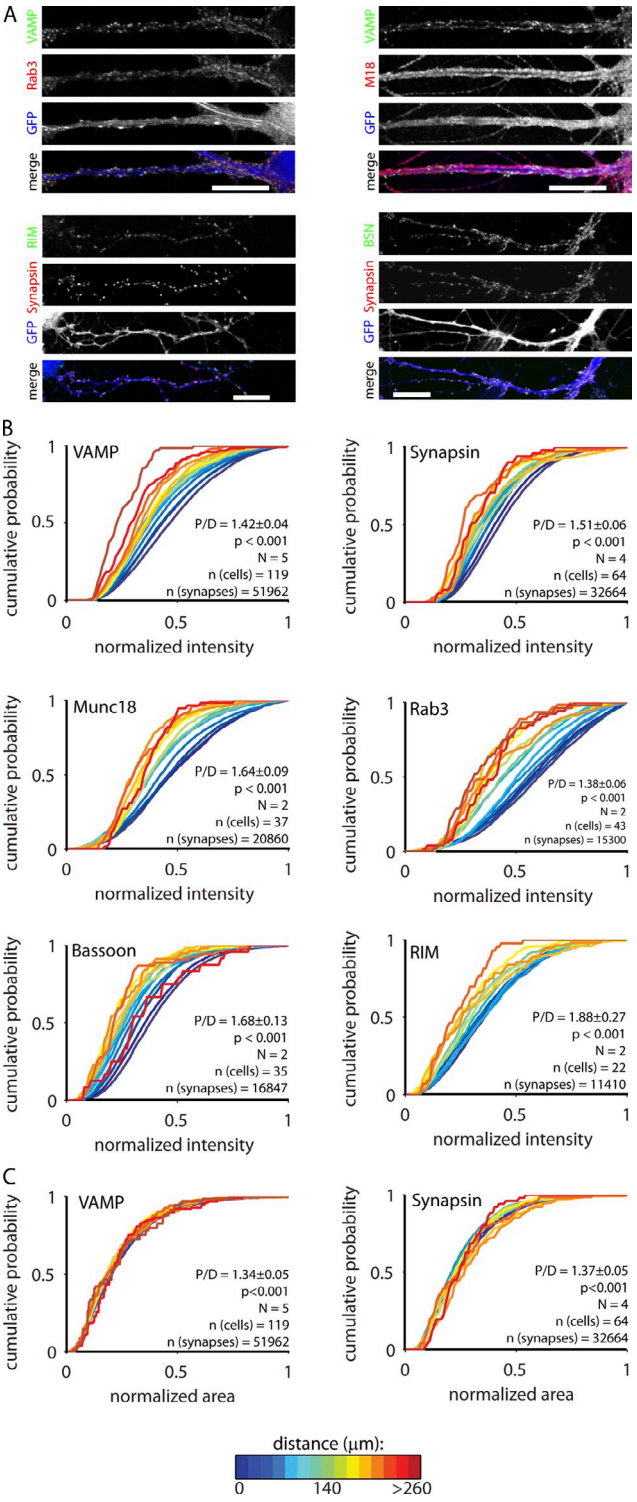

Figure 5. **Autaptic islands display distance-dependent decline in presynaptic protein levels.** (A) Example images of hippocampal autaptic cultures stained for synapse marker Synapsin or VAMP and additional synaptic proteins. GFP expression (delivered with lentivirus) was used as a dendritic marker. Bars, 20 µm. (B) Cumulative histograms of the synaptic intensity of proteins involved in vesicle release. Synapses were grouped based on their distance from the postsynaptic soma. All intensities were normalized to the largest value per cell. P/D is the ratio of proximal (<50 µm) over distal (last 60 µm), and p-value is the significance of the P/D ratio. N represents the number of independent experiments. (C) Surface area of synapsin and VAMP puncta. BSN, Bassoon; M18, Munc18; RIM, Rab3-interacting molecule.

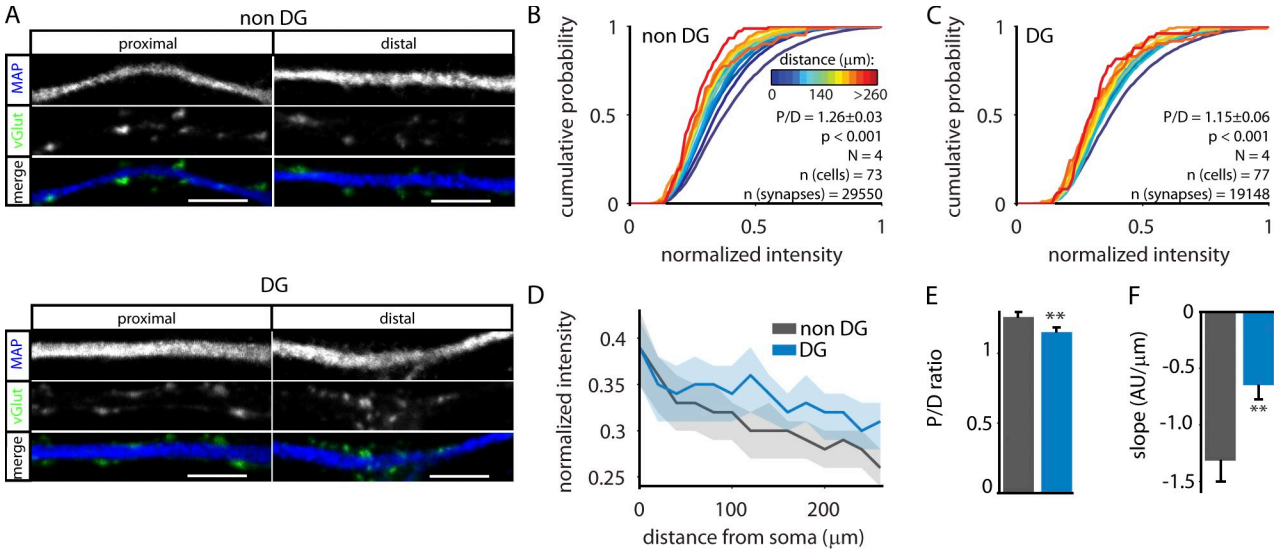

Figure 6. **Strongly reduced distance-dependent scaling in DG cells.** (A) Example images of proximal and distal synapses in DG and non-DG cells. Bars, 5 µm. (B) Cumulative histograms of normalized vGlut intensity of non-DG cells. vGlut intensity was normalized to the largest synapse per cell. P/D is the ratio of proximal (<50 µm) over distal (last 50 µm), and p-value is the significance of the P/D ratio. N represents the number of independent experiments. (C) As in B, for DG cells. (D) Comparison of the histograms in B and C. Solid line represents the median, and the shaded area shows the 0.4–0.6 boundaries. (E) P/D ratio of vGlut intensity of DG and non-DG cells. (F) Mean slopes of linear line fits through data from individual neurons. Error bars represent means ± SEM. **, P < 0.01. AU, arbitrary unit.

of the methods used here. Our results also clearly illustrate that, besides synapse position, other factors are involved in the regulation of presynaptic strength. The identity and activity of the presynaptic cell as well the activation of intracellular signal transduction pathways are factors known to be involved in the regulation of presynaptic vesicle release (Atwood and Karunanithi, 2002; de Jong and Verhage, 2009). In a recent study, it was found that terminals formed by the distal part of the axon were stronger compared with proximal synapses, suggesting that presynaptic strength might also depend on the axonal position of a terminal (Peng et al., 2012). Collectively, the observed p_r of a given synapse is the result of all the aforementioned determinants and cannot be solely attributed to a single factor.

Distance-dependent scaling is dictated by the postsynaptic cell

The synapses studied here are formed by axons from several neighboring neurons. Thus, each axon is capable of determining the location of a synapse on the dendritic tree and to set its presynaptic strength accordingly. It is therefore most likely that the postsynaptic cell dictates the distance-dependent scaling of presynaptic strength, by indicating the position of the synapse on the dendrite via retrograde messenger or cell adhesion molecules. In contrast to known forms of homeostatic plasticity (Turrigiano, 2008; Pozo and Goda, 2010), distance-dependent scaling is independent of neuronal activity (Figs. 4 and 5). Therefore, this retrograde signaling to tune presynaptic strength is most likely distinct from the previously documented, activity-dependent signaling pathways (Regehr et al., 2009). We postulate that, in parallel to local homeostatic mechanisms, presynaptic strength is determined by cell-wide, distance-dependent scaling, which is controlled by the postsynaptic cell (Fig. 7). Distance-dependent scaling might act as a global, default rule, which is stable over time and insensitive to activity in the neuronal network. Homeostatic mechanisms, in turn, respond to changes in neuronal activity and tune individual synapses based on their synaptic use. Together, distance-dependent and homeostatic mechanisms ensure the proper integration of synaptic input with optimal use of metabolic resources (Branco and Staras, 2009).

Distance-dependent scaling is cell type specific

Our results indicate that the gradient of presynaptic strength is the opposite of the previously observed distance-dependent increase in postsynaptic gain in hippocampal pyramidal cells (Magee and Cook, 2000; Losonczy and Magee, 2006). The location-specific integration rules for synaptic input are thought to be of high importance for information processing and memory storage in these cells (Sjöström et al., 2008). Many of these rules, however, are specific for particular cell types (compare, for instance, Williams and Stuart [2002] and Magee and Cook [2000]). Importantly, DG cells were shown to integrate synaptic input differently compared with hippocampal pyramidal cells (Krueppel et al., 2011). The absence of dendritic spikes and the strong attenuation of both EPSPs and back-propagating APs result in a linear summation of synaptic input in DG granule neurons, with similar gain for proximal and distal synapses. It was estimated that DG cells require input from ∼55 synapses to reach their AP threshold compared with only five synchronous EPSPs in hippocampal pyramidal cells (Krueppel et al., 2011). A reduction of presynaptic strength as a function of distance would further reduce the AP firing probability caused by physiological presynaptic activity. By comparing DG and non-DG neurons, we found that, comparable with postsynaptic gain, the distance-dependent scaling of presynaptic strength was significantly reduced in DG cells (Figs. 6 and S3).

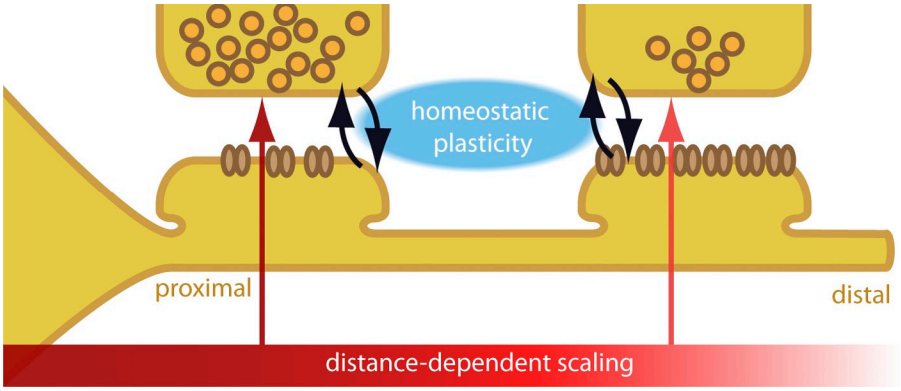

Figure 7. **Pre- and postsynaptic strength is determined by several independent mechanisms.** Chronic changes in synaptic activity lead to compensatory adaptations in synaptic strength (homeostatic plasticity). These mechanisms act locally, at the level of individual synapses. On top of this, the strength of the pre- and postsynapse is scaled in a cell-wide manner, based on the synapse's position on the dendritic tree (distance-dependent scaling). Both mechanisms act in parallel, most likely via independent molecular mechanisms. The distance-dependent scaling is cell type specific and may act in conjunction with the integration rules of the cell's dendritic tree.

The location-specific scaling of presynaptic terminals thus was different between different populations of neurons. This illustrates that distance-dependent scaling of presynaptic strength is a cell type specific property, and neurons appear to tune the strength of their afferent input in conjunction with the cell type–specific integration rules of their dendritic tree.

Distance-dependent scaling is expected to regulate complex network performance

Our data reveal a new rule that regulates the strength of presynaptic terminals formed along the dendritic tree of hippocampal neurons. Because synaptic integration rules are highly dependent on dendritic location (Sjöström et al., 2008), this may be of crucial importance for the proper integration of synaptic activity. In the intact hippocampus, different regions of the dendritic tree receive inputs from different anatomical sources (Spruston and McBain, 2007). Combined with our data, it can be predicted that these inputs differ in presynaptic strength (and probably also STP) based on their dendritic location. In line with this prediction, Ahmed and Siegelbaum (2009) showed that the perforant path (which projects on distal dendrites of CA1 pyramidal cells) displays a low p_r and paired-pulse facilitation, whereas Schaffer collaterals, projecting on proximal dendrites, have a higher p_r and show frequency depression (also see Speed and Dobrunz, 2009). Together with the postsynaptic scaling previously described (Magee and Cook, 2000; Losonczy and Magee, 2006), these distance-dependent rules imply that the power of these anatomical sources to influence the activity of a target neuron depends on the position of their terminals on the dendrite they project on. To what extent distance-dependent scaling affects the strength of other inputs and how this influences information processing in the hippocampus remain important open questions.

Materials and methods

Cell culture and transfection

Dissociated hippocampal cultures were obtained from newborn rats as described previously (de Wit et al., 2009). In brief, hippocampi were dissected in HBBS (Invitrogen) supplemented with 7 mM Hepes and digested with 0.25% trypsin (Invitrogen) at 37°C for 20 min. After trituration with a fire-polished glass pipette, cells were plated at a density of 60,000 cells/well on top of a pregrown rat glia monolayer on 25-mm coverslips. Cultures were grown in Neurobasal supplemented with B27, 18 mM Hepes, 0.5 mM GlutaMAX, and penicillin/streptomycin (all obtained from Invitrogen), and half the medium was replaced once every week. 5 µM arabinofuranosyl cytidine was added at DIV 2 to prevent microglia proliferation. For live-imaging experiments, neurons were transfected with SypHy (gift from A. Jeromin, Allen Institute for Brain Science, Seattle, WA; Granseth et al., 2006) and ECFP at DIV 6–8 using Ca^{2+} phosphate (Köhrmann et al., 1999). The ECFP signal was used to identify the transfected cell. The transfection protocol was optimized to yield only a few transfected cells per coverslip. Autaptic island cultures were cultured similarly as previously described in Wierda et al. (2007). Islands of collagen/poly-D-lysine substrate were applied to glass coverslips using a stamp with evenly spaced squares. Astrocytes were cultured on these islands for 4–7 d before the addition of neurons. Cultures were infected with GFP as a morphological marker, which was delivered with lentivirus at DIV 9.

Electrophysiology and live-cell imaging

Whole-cell recordings were performed at DIV 12–15 with borosilicate glass pipettes (2–4 mOhm) containing 125 mM K^+-gluconic acid, 10 mM NaCl, 4.6 mM $MgCl_2$, 4 mM K_2-ATP, 15 mM creatine phosphate, 1 mM EGTA, and 20 U/ml phosphocreatine kinase, pH 7.3. Intracellular solution for the postsynaptic cell contained 80 µm of fixable Alexa Fluor 468–dextran (Invitrogen). Samples were constantly superfused with external solution containing 2 mM $CaCl_2$, 2.5 mM KCl, 119 mM NaCl, 2 mM $MgCl_2$, 30 mM glucose, and 25 mM Hepes, pH 7.4. Cells were kept in a voltage clamp (membrane potential = −70 mV) using amplifiers (Axopatch 200B; Axon Instruments). APs were induced by 1–2-ms steps to 30 mV, which was controlled by a stimulator (Master-8; A.M.P.I.). Signals were recorded with Digidata 1440A and pCLAMP 10 software (both obtained from Axon Instruments). All experiments were performed at RT (20–23°C).

Imaging was performed using an inverted microscope (IX71; Olympus) using a 40× oil objective, NA 1.41, a xenon lamp (DG-4; Sutter Instrument), and 488/6- and 520/35-nm filter sets (Semrock). Images were acquired with an intensified charge-coupled device camera (XR/TURBO-120EX; Stanford Photonics) at 60 Hz controlled by Piper v1.51 (Stanford Photonics). Regions of interest of 2.2 × 2.2 µm were placed based on the response to 900 APs at 20 Hz with subsequent application of 50 mM NH_4^+ and were omitted from further analyses when they did not respond to this AP train (response of <2× SD of baseline). Raw traces were extracted from the images using ImageJ (National Institutes of Health) and analyzed with custom-written programs in Matlab R2010b (MathWorks). A running mean of 10 frames was applied to the raw traces to reduce noise. Cell pairs were rejected if the imaging results showed substantial activity asynchronous to the applied AP pattern, as it suggests that the SypHy+ synapses were formed by more than one transfected cell. At the end of the experiment, samples were fixed in 4% formaldehyde. The recorded cells were relocated on a confocal microscope (LSM510; Carl Zeiss) to identify the SypHy+ synapses that were formed on the postsynaptic cell.

Immunocytochemistry and confocal microscopy

Cultures were fixed at DIV 14 (unless otherwise stated) with 4% formaldehyde and permeabilized with 0.5% Triton X-100. Neurons were then stained with primary antibodies for 1 h at RT, washed with PBS, and stained for 1 h at RT with secondary antibodies with conjugated Alexa Fluor (1:1,000; Invitrogen). The primary antibodies and dilution used were chicken anti-MAP (1:10,000; Abcam), mouse anti-VAMP2 (1:1,000; Synaptic Systems), rabbit anti-Synapsin I (1:1,000; P610; a gift from T.C. Sudhof, Stanford University School of Medicine, Stanford, CA), mouse anti-Bassoon (1:500; Stressgene), mouse anti–Munc18-1 (1:500; Synaptic Systems), mouse anti–Rab3-interacting molecule (1:200; BD), rabbit anti-Syntaxin (1:1,000; Synaptic Systems),

rabbit anti-vGAT (1:500; Synaptic Systems), rabbit anti-Prox1 (1:5,000; Covance), rabbit anti-vGlut1 (1:500; Synaptic Systems), guinea pig anti-vGlut1 (used in combination with Prox1; 1:5,000; Millipore), and rabbit anti–Synaptotagmin-1 (1:2,000; W855; a gift from T.C. Sudhof). Coverslips were mounted with 1,4-diazobicyclo-[2.2.2]-octane–Mowiol (Invitrogen) and examined on a confocal microscope (LSM510). Images were acquired with a 40× oil objective, NA 1.3, and 0.7× mechanical zoom as z stacks with a 1-µm interval. Images were collapsed to maximal projection and analyzed in Matlab with SynD (Schmitz et al., 2011) and custom-written programs. Synapses were detected based on the staining for VAMP, Synapsin, vGAT, or vGlut, depending on antibody compatibility. Detected regions were subsequently used to measure the synaptic intensity of additional proteins. Arc distance from the soma was measured along the dendritic marker MAP. For distance-binned cumulative histograms, synapses were grouped based on distance from postsynaptic soma in 20-µm bins. Fluorescence intensity was normalized to the brightest synapse formed on each neuron.

Statistics

To test the distance dependency of the measured parameters per cell, the ratio of proximal synapses (<50 µm from the soma) over distal synapses (last 50 µm) was calculated per cell (P/D ratio). Significance of this ratio was tested with a one-sample Wilcoxon rank test, assuming that P/D = 1 if the measured parameter is independent of distance. Statistical significance between experimental groups was tested using a Kruskal-Wallis analysis of variance. All tests were performed in Matlab. N indicates the number of independent experiments. Differences were considered significant if $P < 0.05$. All bar graphs represent means ± SEM.

Chemicals

TTX and AP5 were obtained from Ascent, and DNQX was purchased from Enzo Life Sciences. All other chemicals were obtained from Sigma-Aldrich.

Online supplemental material

Fig. S1 describes the comparison of distance-dependent scaling in cells cultured for 2 or 3 wk. Fig. S2 illustrates the relationship between the total vesicle pool size and the size of the RRP. Fig. S3 contains the morphological analysis of DG and non-DG cells. Online supplemental material is available at http://www.jcb.org/cgi/content/full/jcb.201112135/DC1.

We would like to thank Hans Lodder and Jurjen Broeke for their invaluable technical assistance, Boukje Beuger and Desiree Schut for their help with cell culture, and the other members of the Verhage laboratory for helpful discussions.

This work was supported by the European Union (EUSynapse project 019055 to M. Verhage, EUROSPIN project HEALTH-F2-2009-241498 to M. Verhage, and a SynSys project HEALTH-F2-2009-242167 to M. Verhage), the Netherlands Organization for Scientific Research, Netherlands Organisation for Scientific Research (Pionier/VICI900-01-001 and Netherlands Organisation for Health Research and Development 903-42-095 to M. Verhage), and the Neuro-Bsik Mouse Phenomics Consortium (BSIK03053). S.K. Schmitz is supported by the Netherlands Organisation for Scientific Research (TopTalent 021.001.076) and Neuromics Marie Curie Early stage Training Grant (MEST-CT-2005-020919).

Author contributions: A.P.H. de Jong, R.F.G. Toonen, and M. Verhage designed research, A.P.H. de Jong performed immunocytochemistry and live-imaging experiments, S.K. Schmitz performed autapse experiments, A.P.H. de Jong analyzed the data, and A.P.H. de Jong and M. Verhage wrote the manuscript.

Submitted: 23 December 2011
Accepted: 14 March 2012

References

Abbott, L.F., and W.G. Regehr. 2004. Synaptic computation. *Nature*. 431:796–803. http://dx.doi.org/10.1038/nature03010

Ahmed, M.S., and S.A. Siegelbaum. 2009. Recruitment of N-Type Ca(2+) channels during LTP enhances low release efficacy of hippocampal CA1 perforant path synapses. *Neuron*. 63:372–385. http://dx.doi.org/10.1016/j.neuron.2009.07.013

Atwood, H.L., and S. Karunanithi. 2002. Diversification of synaptic strength: presynaptic elements. *Nat. Rev. Neurosci.* 3:497–516. http://dx.doi.org/10.1038/nrn876

Bagri, A., T. Gurney, X. He, Y.R. Zou, D.R. Littman, M. Tessier-Lavigne, and S.J. Pleasure. 2002. The chemokine SDF1 regulates migration of dentate granule cells. *Development*. 129:4249–4260.

Balaji, J., and T.A. Ryan. 2007. Single-vesicle imaging reveals that synaptic vesicle exocytosis and endocytosis are coupled by a single stochastic mode. *Proc. Natl. Acad. Sci. USA*. 104:20576–20581. http://dx.doi.org/10.1073/pnas.0707574105

Baranes, D., J.C. López-García, M. Chen, C.H. Bailey, and E.R. Kandel. 1996. Reconstitution of the hippocampal mossy fiber and associational-commissural pathways in a novel dissociated cell culture system. *Proc. Natl. Acad. Sci. USA*. 93:4706–4711. http://dx.doi.org/10.1073/pnas.93.10.4706

Bekkers, J.M., and C.F. Stevens. 1991. Excitatory and inhibitory autaptic currents in isolated hippocampal neurons maintained in cell culture. *Proc. Natl. Acad. Sci. USA*. 88:7834–7838. http://dx.doi.org/10.1073/pnas.88.17.7834

Branco, T., and M. Häusser. 2011. Synaptic integration gradients in single cortical pyramidal cell dendrites. *Neuron*. 69:885–892. http://dx.doi.org/10.1016/j.neuron.2011.02.006

Branco, T., and K. Staras. 2009. The probability of neurotransmitter release: variability and feedback control at single synapses. *Nat. Rev. Neurosci.* 10:373–383. http://dx.doi.org/10.1038/nrn2634

Branco, T., K. Staras, K.J. Darcy, and Y. Goda. 2008. Local dendritic activity sets release probability at hippocampal synapses. *Neuron*. 59:475–485. http://dx.doi.org/10.1016/j.neuron.2008.07.006

Branco, T., V. Marra, and K. Staras. 2010. Examining size-strength relationships at hippocampal synapses using an ultrastructural measurement of synaptic release probability. *J. Struct. Biol.* 172:203–210. http://dx.doi.org/10.1016/j.jsb.2009.10.014

Burrone, J., Z. Li, and V.N. Murthy. 2006. Studying vesicle cycling in presynaptic terminals using the genetically encoded probe synaptopHluorin. *Nat. Protoc.* 1:2970–2978. http://dx.doi.org/10.1038/nprot.2006.449

Claiborne, B.J., D.G. Amaral, and W.M. Cowan. 1990. Quantitative, three-dimensional analysis of granule cell dendrites in the rat dentate gyrus. *J. Comp. Neurol.* 302:206–219. http://dx.doi.org/10.1002/cne.903020203

de Jong, A.P., and M. Verhage. 2009. Presynaptic signal transduction pathways that modulate synaptic transmission. *Curr. Opin. Neurobiol.* 19:245–253. http://dx.doi.org/10.1016/j.conb.2009.06.005

de Wit, J., R.F. Toonen, and M. Verhage. 2009. Matrix-dependent local retention of secretory vesicle cargo in cortical neurons. *J. Neurosci.* 29:23–37. http://dx.doi.org/10.1523/JNEUROSCI.3931-08.2009

Dobrunz, L.E., and C.F. Stevens. 1997. Heterogeneity of release probability, facilitation, and depletion at central synapses. *Neuron*. 18:995–1008. http://dx.doi.org/10.1016/S0896-6273(00)80338-4

Fernandez-Alfonso, T., and T.A. Ryan. 2008. A heterogeneous "resting" pool of synaptic vesicles that is dynamically interchanged across boutons in mammalian CNS synapses. *Brain Cell Biol.* 36:87–100. http://dx.doi.org/10.1007/s11068-008-9030-y

Granseth, B., B. Odermatt, S.J. Royle, and L. Lagnado. 2006. Clathrin-mediated endocytosis is the dominant mechanism of vesicle retrieval at hippocampal synapses. *Neuron*. 51:773–786. http://dx.doi.org/10.1016/j.neuron.2006.08.029

Herzog, E., F. Nadrigny, K. Silm, C. Biesemann, I. Helling, T. Bersot, H. Steffens, R. Schwartzmann, U.V. Nägerl, S. El Mestikawy, et al. 2011. In vivo imaging of intersynaptic vesicle exchange using VGLUT1 Venus knock-in mice. *J. Neurosci.* 31:15544–15559. http://dx.doi.org/10.1523/JNEUROSCI.2073-11.2011

Jiang, X., P.E. Litkowski, A.A. Taylor, Y. Lin, B.J. Snider, and K.L. Moulder. 2010. A role for the ubiquitin-proteasome system in activity-dependent presynaptic silencing. *J. Neurosci.* 30:1798–1809. http://dx.doi.org/10.1523/JNEUROSCI.4965-09.2010

Jockusch, W.J., D. Speidel, A. Sigler, J.B. Sørensen, F. Varoqueaux, J.S. Rhee, and N. Brose. 2007. CAPS-1 and CAPS-2 are essential synaptic vesicle priming proteins. *Cell*. 131:796–808. http://dx.doi.org/10.1016/j.cell.2007.11.002

Koester, H.J., and D. Johnston. 2005. Target cell-dependent normalization of transmitter release at neocortical synapses. *Science*. 308:863–866. http://dx.doi.org/10.1126/science.1100815

Köhrmann, M., W. Haubensak, I. Hemraj, C. Kaether, V.J. Lessmann, and M.A. Kiebler. 1999. Fast, convenient, and effective method to transiently transfect primary hippocampal neurons. *J. Neurosci. Res.* 58:831–835. http://dx.doi.org/10.1002/(SICI)1097-4547(19991215)58:6<831::AID-JNR10>3.0.CO;2-M

Kress, G.J., M.J. Dowling, J.P. Meeks, and S. Mennerick. 2008. High threshold, proximal initiation, and slow conduction velocity of action potentials in dentate granule neuron mossy fibers. *J. Neurophysiol.* 100:281–291. http://dx.doi.org/10.1152/jn.90295.2008

Krueppel, R., S. Remy, and H. Beck. 2011. Dendritic integration in hippocampal dentate granule cells. *Neuron*. 71:512–528. http://dx.doi.org/10.1016/j.neuron.2011.05.043

Laviv, T., I. Riven, I. Dolev, I. Vertkin, B. Balana, P.A. Slesinger, and I. Slutsky. 2010. Basal GABA regulates GABA(B)R conformation and release

probability at single hippocampal synapses. *Neuron*. 67:253–267. http://dx.doi.org/10.1016/j.neuron.2010.06.022

Lazarevic, V., C. Schöne, M. Heine, E.D. Gundelfinger, and A. Fejtova. 2011. Extensive remodeling of the presynaptic cytomatrix upon homeostatic adaptation to network activity silencing. *J. Neurosci.* 31:10189–10200. http://dx.doi.org/10.1523/JNEUROSCI.2088-11.2011

Losonczy, A., and J.C. Magee. 2006. Integrative properties of radial oblique dendrites in hippocampal CA1 pyramidal neurons. *Neuron*. 50:291–307. http://dx.doi.org/10.1016/j.neuron.2006.03.016

Magee, J.C., and E.P. Cook. 2000. Somatic EPSP amplitude is independent of synapse location in hippocampal pyramidal neurons. *Nat. Neurosci.* 3:895–903. http://dx.doi.org/10.1038/78800

Matz, J., A. Gilyan, A. Kolar, T. McCarvill, and S.R. Krueger. 2010. Rapid structural alterations of the active zone lead to sustained changes in neurotransmitter release. *Proc. Natl. Acad. Sci. USA*. 107:8836–8841. http://dx.doi.org/10.1073/pnas.0906087107

Miesenböck, G., D.A. De Angelis, and J.E. Rothman. 1998. Visualizing secretion and synaptic transmission with pH-sensitive green fluorescent proteins. *Nature*. 394:192–195. http://dx.doi.org/10.1038/28190

Murthy, V.N., T.J. Sejnowski, and C.F. Stevens. 1997. Heterogeneous release properties of visualized individual hippocampal synapses. *Neuron*. 18: 599–612. http://dx.doi.org/10.1016/S0896-6273(00)80301-3

Murthy, V.N., T. Schikorski, C.F. Stevens, and Y. Zhu. 2001. Inactivity produces increases in neurotransmitter release and synapse size. *Neuron*. 32:673–682. http://dx.doi.org/10.1016/S0896-6273(01)00500-1

Mutch, S.A., P. Kensel-Hammes, J.C. Gadd, B.S. Fujimoto, R.W. Allen, P.G. Schiro, R.M. Lorenz, C.L. Kuyper, J.S. Kuo, S.M. Bajjalieh, and D.T. Chiu. 2011. Protein quantification at the single vesicle level reveals that a subset of synaptic vesicle proteins are trafficked with high precision. *J. Neurosci.* 31:1461–1470. http://dx.doi.org/10.1523/JNEUROSCI.3805-10.2011

Pelkey, K.A., L. Topolnik, J.C. Lacaille, and C.J. McBain. 2006. Compartmentalized Ca(2+) channel regulation at divergent mossy-fiber release sites underlies target cell-dependent plasticity. *Neuron*. 52:497–510. http://dx.doi.org/10.1016/j.neuron.2006.08.032

Peng, X., T.D. Parsons, and R.J. Balice-Gordon. 2012. Determinants of synaptic strength vary across an axon arbor. *J. Neurophysiol.*

Pozo, K., and Y. Goda. 2010. Unraveling mechanisms of homeostatic synaptic plasticity. *Neuron*. 66:337–351. http://dx.doi.org/10.1016/j.neuron.2010.04.028

Regehr, W.G., M.R. Carey, and A.R. Best. 2009. Activity-dependent regulation of synapses by retrograde messengers. *Neuron*. 63:154–170. http://dx.doi.org/10.1016/j.neuron.2009.06.021

Reyes, A., R. Lujan, A. Rozov, N. Burnashev, P. Somogyi, and B. Sakmann. 1998. Target-cell-specific facilitation and depression in neocortical circuits. *Nat. Neurosci.* 1:279–285. http://dx.doi.org/10.1038/1092

Scanziani, M., B.H. Gähwiler, and S. Charpak. 1998. Target cell-specific modulation of transmitter release at terminals from a single axon. *Proc. Natl. Acad. Sci. USA*. 95:12004–12009. http://dx.doi.org/10.1073/pnas.95.20.12004

Schikorski, T., and C.F. Stevens. 2001. Morphological correlates of functionally defined synaptic vesicle populations. *Nat. Neurosci.* 4:391–395. http://dx.doi.org/10.1038/86042

Schmitz, S.K., J.J. Hjorth, R.M. Joemai, R. Wijntjes, S. Eijgenraam, P. de Bruijn, C. Georgiou, A.P. de Jong, A. van Ooyen, M. Verhage, et al. 2011. Automated analysis of neuronal morphology, synapse number and synaptic recruitment. *J. Neurosci. Methods*. 195:185–193. http://dx.doi.org/10.1016/j.jneumeth.2010.12.011

Seress, L., and J. Pokorny. 1981. Structure of the granular layer of the rat dentate gyrus. A light microscopic and Golgi study. *J. Anat.* 133:181–195.

Shigemoto, R., A. Kulik, J.D. Roberts, H. Ohishi, Z. Nusser, T. Kaneko, and P. Somogyi. 1996. Target-cell-specific concentration of a metabotropic glutamate receptor in the presynaptic active zone. *Nature*. 381:523–525. http://dx.doi.org/10.1038/381523a0

Sjöström, P.J., E.A. Rancz, A. Roth, and M. Häusser. 2008. Dendritic excitability and synaptic plasticity. *Physiol. Rev.* 88:769–840. http://dx.doi.org/10.1152/physrev.00016.2007

Slutsky, I., S. Sadeghpour, B. Li, and G. Liu. 2004. Enhancement of synaptic plasticity through chronically reduced Ca2+ flux during uncorrelated activity. *Neuron*. 44:835–849. http://dx.doi.org/10.1016/j.neuron.2004.11.013

Smith, M.A., G.C. Ellis-Davies, and J.C. Magee. 2003. Mechanism of the distance-dependent scaling of Schaffer collateral synapses in rat CA1 pyramidal neurons. *J. Physiol.* 548:245–258. http://dx.doi.org/10.1113/jphysiol.2002.036376

Speed, H.E., and L.E. Dobrunz. 2009. Developmental changes in short-term facilitation are opposite at temporoammonic synapses compared to Schaffer collateral synapses onto CA1 pyramidal cells. *Hippocampus*. 19:187–204. http://dx.doi.org/10.1002/hipo.20496

Spruston, N., and C.J. McBain. 2007. Structural and functional properties of hippocampal neurons. *In* The Hippocampus Book. P. Andersen, R. Morris, D.G. Amaral, T. Bliss, and J. O'Keefe, editors. Oxford University Press, Oxford/New York. 133–201.

Sudhof, T.C. 2004. The synaptic vesicle cycle. *Annu. Rev. Neurosci.* 27:509–547. http://dx.doi.org/10.1146/annurev.neuro.26.041002.131412

Tong, G., R.C. Malenka, and R.A. Nicoll. 1996. Long-term potentiation in cultures of single hippocampal granule cells: a presynaptic form of plasticity. *Neuron*. 16:1147–1157. http://dx.doi.org/10.1016/S0896-6273(00)80141-5

Toonen, R.F., K. Wierda, M.S. Sons, H. de Wit, L.N. Cornelisse, A. Brussaard, J.J. Plomp, and M. Verhage. 2006. Munc18-1 expression levels control synapse recovery by regulating readily releasable pool size. *Proc. Natl. Acad. Sci. USA*. 103:18332–18337. http://dx.doi.org/10.1073/pnas.0608507103

Turrigiano, G.G. 2008. The self-tuning neuron: synaptic scaling of excitatory synapses. *Cell*. 135:422–435. http://dx.doi.org/10.1016/j.cell.2008.10.008

Welzel, O., C.H. Tischbirek, J. Jung, E.M. Kohler, A. Svetlitchny, A.W. Henkel, J. Kornhuber, and T.W. Groemer. 2010. Synapse clusters are preferentially formed by synapses with large recycling pool sizes. *PLoS ONE*. 5:e13514. http://dx.doi.org/10.1371/journal.pone.0013514

Wierda, K.D., R.F. Toonen, H. de Wit, A.B. Brussaard, and M. Verhage. 2007. Interdependence of PKC-dependent and PKC-independent pathways for presynaptic plasticity. *Neuron*. 54:275–290. http://dx.doi.org/10.1016/j.neuron.2007.04.001

Williams, M.E., S.A. Wilke, A. Daggett, E. Davis, S. Otto, D. Ravi, B. Ripley, E.A. Bushong, M.H. Ellisman, G. Klein, and A. Ghosh. 2011. Cadherin-9 regulates synapse-specific differentiation in the developing hippocampus. *Neuron*. 71:640–655. http://dx.doi.org/10.1016/j.neuron.2011.06.019

Williams, S.R., and G.J. Stuart. 2002. Dependence of EPSP efficacy on synapse location in neocortical pyramidal neurons. *Science*. 295:1907–1910. http://dx.doi.org/10.1126/science.1067903